

**Association of clonal hematopoiesis and AITL: genetic evidence for stem cell origin, etiology and prediction of secondary hematologic malignancy in AITL**

Shuhua Cheng<sup>1</sup>, Wei Zheng<sup>2</sup>, Giorgio Inghirami<sup>1</sup>, Wayne Tam<sup>1\*</sup>

<sup>1</sup>Department of Pathology and Laboratory Medicine, <sup>2</sup> Genomics Resources Core Facility, Weill Cornell Medicine, New York, NY 10021

**Supplemental Text**

### **Fig.1A: 6 illustrative cases in which common mutated HSC developed into CH and AITL or PTCL-NOS**

In Patient #1, identical *TET2* and *DNMT3A* somatic mutations, p. E1089fs and p.F791L, were identified both in CH (VAFs: 48.39%, 34.62%) and in the neoplastic T cells in the diagnostic LN specimen (VAFs: 36.87%, 27.59%) (**Figure 1A**). The other four pathogenic variants, *TET2* p.Q743\*, *RHOA* p.G17V, *IDH2* p.R172T and *PTPRF* p.R654H, were detected at high VAFs in the LN but at much lower VAFs in the BM (**Figure 1A**). These results demonstrate that the latter four mutations are likely acquired at a later time point during AITL development (late mutations) and the low-VAF variants detected in the BM represent minimal involvement in the BM and not CH. Patient #4 had no overt evidence of a myeloid neoplasm in the BM while diagnosed with AITL, and had 2.1% bone marrow involvement by AITL according to immunophenotypic and gene rearrangement studies. The T cell NGS panel identified 7 pathogenic mutations in the primary lymphoma, of which 6 were also found in the matched BM. The allelic burden of the two mutations with the highest VAFs (*DNMT3A* p. Q678\*, VAF=6.22%; *ATPIA3* p.V216M, VAF=4.47%), were 2 to 3 times that of the estimated tumor burden (2.1%) in the BM, suggesting that *DNMT3A* p. Q678\* and *ATPIA3* p.V216M were not only present in the neoplastic T-cells but also associated with CH. The other 5 mutations, including *RHOA* p.G17V and *IDH2* p. R172G, were found at the VAFs ranging from 0% to 1.5% in the BM, consistent with lymphoma involvement rather than CH. These results suggest that these 5 mutations were acquired subsequent to the CH-associated mutations described above. Interestingly, sequencing a relapsed lymphoma specimen from this case identified only one mutation *DNMT3A* p. Q678\*. This mutation information in the relapsed lymphoma helps clarify the clonal architecture of both the primary AITL and CH. First, it suggests that the primary AITL harbored two clones, a dominant clone with *ATPIA3*, *DLGAP3*, *TET2*, *RHOA* and *IDH2* mutations, and a minor clone with *DNMT3A* mutation, the latter being the precursor clone for relapse. Second, it also implies that there are 2 clones in CH, one associated with the *DNMT3A* mutation and the other with the *ATPIA3* mutation. In Patient #10, the CH-associated variant shared between the primary lymphoma and the matched BM, *TET2* p. N1484K, was identified at high allelic burden in both the lymphoma and BM samples (VAFs in LN vs BM, 47.33% vs 38.26%). Another *TET2* mutation, p. D1378G, was also identified in the both the LN and the BM, at VAFs of 16.89% and 0.32% respectively. The large difference of the VAF in the BM of the two *TET2* mutations suggests that they may belong to different HSC clones, each of which has markedly different CH contribution, or the *TET2* p.D1378G mutation was acquired subsequent to the *TET2* p.N1484K mutation as a subclonal mutation in the HSC. The other 3 mutations: *TET2* p.V415fs, *RHOA* p.G17V and *IDH2* p.R172T were present exclusively in the lymphoma sample. In patient #29, the *DNMT3A* R882H hot-spot mutation was shared at high VAFs in both the lymphoma and BM (46% and 35.6%), consistent with a CH-associated mutation, while the other 4 mutations detected in the LN was present in the BM at low VAFs, consistent with BM involvement by T-cell lymphoma. Interestingly, both the *TET2* N1484K mutation in patient #10 and the *DNMT3A* R882H mutation in patient #29 were present in the primary lymphomas at a VAF of close to 50%, about 3-4 times the allelic fractions of other mutations identified in the LN. This finding implies the presence of these mutations in almost the entire cell population in the LN. However, based on immunomorphologic evaluation and the VAF of the other mutations identified in the LN, the tumor burden in the LN for these two cases is about 20-40%. This raises the possibility that besides the neoplastic T cells, reactive lymphocytes in these two cases might also harbor the CH-associated mutations.

In the two PTCL-NOS cases (#2 and #18), we observed similar findings as described above for AITL (**Fig. 1A**). Patient #2 showed eosinophilia with 1.5% neoplastic T cells involvement in the BM. Two pathogenic *STAT3* mutations were identified. One could be considered a CH-associated mutation (*STAT3* p.Y657\_K658insALL, VAFs in LN vs BM, 21.61% vs 8.34%) since its VAF is considerably higher than the estimated percentage of tumor involvement in the BM. The other is most likely PTCL-NOS-related mutation (*STAT3* p.W474\*). This *STAT3* nonsense mutation had the allelic burden of 18.33% in the primary lymphoma but was present at much lower level (VAF = 2%) in the matched PB, in line with the estimated tumor burden. Patient #18 presented mildly hypercellular marrow with mild granulocytic hyperplasia while diagnosed with PTCL-NOS and had no involvement in the BM per the overall pathologic studies. The NGS target panel identified a splice mutation in *TET2* (c.3501-1G>A) and a missense mutation in *SETX* (p. Y2258D) shared between CH and PTCL-NOS. Two mutations (*TP53* p.P151T and *ARID1A* p. G779\*) were only found in the neoplastic T cells, presumably representing later mutations in PTCL-NOS development following acquisition of the *TET2* and *SETX* mutations.

### **Fig. 3: three AITL cases with concurrent hematologic neoplasm**

Patient #5 was initially diagnosed as AITL, followed by a diagnosis of chronic myelomonocytic leukemia (CMML) 7 months later. In the BM specimen, taken four months prior to the diagnosis of CMML and sequenced in this study, the overall pathologic findings showed 1-5% involvement by AITL and suspected involvement by a myeloid neoplasm. Three identical mutations, including 2 *TET2* and one *DNMT3A* mutations: p.I274delinsISfs, p.L1830\* and p.W893S alterations, respectively, were identified in both the LN and BM with high allele burdens (VAF range, 25-50%, **Fig. 3A, Suppl. Table 3**). In addition, pathogenic *SRSF2* and *JAK2* mutations were identified in the BM. These findings support a scenario in which AITL and CMML arose via divergent evolution from a common HSC clone mutated in the CH-associated *TET2* and *DNMT3A* genes. Subsequent development involves accumulation of additional mutations: *SRSF2* and *JAK2* mutations from CH to CMML, and *IDH2* with other mutations to AITL.

Patient #20 was initially diagnosed with PV and progressed to post-PV PMF after 10 years. Two months later, the patient was also diagnosed with AITL. We sequenced the T-cell lymphoma in the LN and the paired bone marrow specimen with post-PV PMF (the initial PV specimen was unavailable). The overall pathologic studies showed no lymphoma involvement in the BM. The NGS sequencing revealed that the T and myeloid malignant cells harbored two identical destructive *TET2* mutations with high mutant allele burdens, p. Q939\* (20% VAF) and p. E1026delinsXDFs (42% VAF). The driver mutation for MPN, *JAK2* p.V617F, was not only present in the post-PV PMF (88% VAF), but also found in the concomitant AITL with the mutant allele burden of 54.5% (**Fig. 3B, Suppl. Table 3**). No *IDH2* or *RHOA* mutation was detected in the AITL. These findings suggest that the *JAK2* driver mutation was acquired early in the HSC. Indeed, *JAK2* mutation was thought to be an early event in PV<sup>1</sup>. In this particular case, the combination of *TET2* and *JAK2* V617F may also be sufficient to drive AITL development, as no other drivers like *IDH2* or *RHOA* were found.

Patient #14 initially presented as immune thrombocytopenia (ITP) and had a splenectomy in 2008. He was diagnosed with AITL two years later and DLBCL about 7 years later. We sequenced two diagnostic tissue samples for the AITL and DLBCL, respectively, as well as one BM sample collected from this patient in 2010. The morphologic, immunophenotyping and molecular findings confirmed that the BM sample was not involved by AITL or a myeloid neoplasm. Interestingly, two nonsense *TET2* mutations, p.K454\* and p.K1799\*, were identified in all three samples with the VAFs ranging from 32% to 51%. An additional pathologic mutation *EZH2*, p. Y646S, was detected only in the DLBCL (**Fig. 3C, Suppl. Table 3**). The results from this patient suggest that the mutated HSC clone, harboring *TET2* p.K454\* and p.K1799\* alterations, differentiates into progeny cells of three different lineages (myeloid, T lymphoid, B lymphoid), each of which gives rise to CH, or transformed to AITL or DLBCL. The additional *EZH2* mutation has been reported in B-cell lymphomas<sup>2,3</sup> and likely plays a role in the DLBCL development.

## Method

### Patients and Study Samples

All tissue samples (27 lymph node tissue specimens, 27 bone marrow aspirate/peripheral blood samples) were collected from 25 AITL or 2 PTCL NOS patients who were diagnosed or confirmed from June 2010 to December 2019 following World Health Organization classification criteria by attending hematopathologists at NYP/Weill Cornell Medical Center, and clinical information was obtained from electronic clinical records. Of these 27 study cases, 4 were initially diagnosed with PTCL with THF phenotype (**Suppl. Table. 1**), and included as the part of the AITL cases according to their similar clinical and molecular features as recently proposed by WHO<sup>4</sup>. This study was conducted in accordance with the Declaration of Helsinki regulations of the protocols approved by the Institutional Review Board of Weill Cornell Medicine, New York, USA. Written consent for use of the samples for research was obtained from patients or their guardians.

Genomic DNA was extracted from lymph node tissue and bone marrow or PBMC cell pellets following manufacturer's instructions (QIAamp DNA Mini Kit, Qiagen, Germantown). DNA samples and sequencing libraries used in targeting sequencing as described below were quantitated by Tape Station (Agilent Technologies, Santa Clara) and Qubit (Thermo Fisher Scientific, Singapore).

### T Cell Targeted Sequencing

A 538 gene targeted sequencing panel were designed to investigate the genomic profile of the primary tumors and the BM/PB tissues<sup>5</sup>. The genomic regions covered by sequencing include coding exons and splice sites of these genes (target region: ~3.2 Mb) that were reported being recurrently mutated (>2) in mature T-cell neoplasms, as well as genomic regions corresponding to recurrent translocations. Using an input of genomic DNA of at least 100 ng isolated from frozen tissues or FFPE samples, the next-generation sequencing (NGS) libraries were constructed using

the KAPA Hyperplus Kit (Roche, Basel, Switzerland), and hybrid selection was performed with the Twist Library Prep Kit (Twist Biosciences, San Francisco, CA, USA), according to the manufacturer's protocols. Multiplexed libraries were sequenced using 150-bp paired end HiSeq4000 sequencers (Illumina, San Diego, CA, USA). NEXTGENE software (Softgenetics, State College, PA, USA) was used to perform bioinformatic analysis (SNV and INDEL variant calls) with standard settings recommended by the manufacturer. Specifically, cutoff values for the variant allele frequency, population frequencies, and strand bias were set at 5%, 0.01%, and 1:5, respectively.

## Myeloid NGS Panel

Targeted enrichment of 45 genes recurrently mutated in myeloid malignancies was performed using the Thunderstorm system with a customized primer panel<sup>6</sup>. The primers target coding exons of the genes, leading to a total of 726 amplicons. Libraries were prepared by microdroplet-based PCR target enrichment method from DNA, followed by sequencing using the Illumina MiSeq yielding 260-bp paired end reads. Sequencing data were analyzed and reported with a customized analytical pipeline. This NGS panel testing is performed in a clinical lab CLIA-certified and accredited by the College of American Pathologists.

## Data Analysis

Data analysis were conducted with GraphPad/Prism 5 software and various R packages, including base packages, ggplot2, ComplexHeatmap and Maftools. The survival comparison was analyzed using Kaplan-Meier curves (log-rank test, significance defined as  $p < 0.05$ ).

## Supplemental figure legend

**Suppl. Fig. 1. AITL variants involving BM/PB.** (A) Venn diagram illustrates the distribution of the shared, and the LN or BM/PB-specific mutations. Note that the variants detected in the BM/PB due to lymphoma involvement are included in this diagram, in contrast to Fig. 1B presented in the main text. (B) The type of variants and mutation frequencies (relative to the total number of cases) for the top 6 mutated genes identified in AITL/PTCL-NOS and matched BM/PB are shown. Different colors represent variant classifications as indicated. (C) Heat map showing the mutations detected in the BM/PB samples in each case. Only the major recurrent mutations are listed. The tumor burden (TB) in the BM/PB was estimated based on morphologic and immunophenotypic and molecular assessment, and the predicted CH status (determined based on comparison of the VAF of the mutations with TB) is indicated. Blue rectangles highlight the VAFs of the variants due to AITL involvement. CH, clonal hematopoiesis; +, presence of CH; -, absence of CH; \$, mutation in *STAT3*; ^, mutation in *DDX11*. (D) Dot plot comparing VAFs of the CH-associated variants and those related to lymphoma involvement in the BM/PB specimens. Mean  $\pm$ SEM of the VAFs is shown for each subgroup. (E) The proportion of the cases with or without BM or PB involvement by the neoplastic T cells (IVS), or with/without clonal hematopoiesis (CH), respectively, is summarized.

**Suppl. Fig.2 Overall and lymphoma-specific genomic alterations in primary AITL/PTCL-NOS.** (A) Mutation plot showing the overall mutation profile in the LN tissues involved by AITL/PTCL-NOS. (B) Mutation plot showing the AITL/PTCL-NOS-specific mutations identified in lymphoma samples after excluding the CH-associated variants. Top bars on each plot indicate the numbers of variants detected per sample. The percentage at right shows the gene mutation frequency in the cohort of the patients. Sample IDs are indicated at the bottom of each plot. Variant classifications are indicated with different colors.

**Suppl. Fig.3 Overall and CH-related genomic alterations in the matched BM/PB samples.** (A) The overall mutation profile in the BM/PB shown. (B) The CH-related mutation profile identified in the BM/PB is shown after excluding the variants due to AITL involvement. Top bars on each plot indicate the numbers of the variants detected per sample. The percentage showing gene mutation frequency in the patient cohort is shown at the right. Sample IDs are indicated at the bottom of each plot. Variant classifications are indicated with different colors.

**Suppl. Fig. 4 Comparison of VAFs of the variants found in paired AITL and BM/PB samples.** Red color highlights the CH-associated variants shared between the LN and BM/PB compartments. The black circles indicate variants specific to the lymphomas, the pink circles represent mutations specific to BM/PB. Cases that were not presented in Fig. 1 and Fig. 3 are shown in this figure. In Pt #7, three mutations specific to BM were found in *PLCG1*, *ACSL3* and *CTTNBP2*. These may represent novel CH-associated mutations. In Pt #8, *DNMT3A* p.W330\*, likely

representing a minor CH clone, was also found specifically in the BM. In Pt.#24, an additional ASXL1 frameshift mutation was identified in the BM, which showed hypercellularity with increased granulopoiesis. In this patient, we appeared to capture the acquisition of a subclonal *JAK2* V617F mutation during tumor progression, which was identified by the myeloid panel in the purified granulocytes from the PB but not detected in the BM one year before (#24).

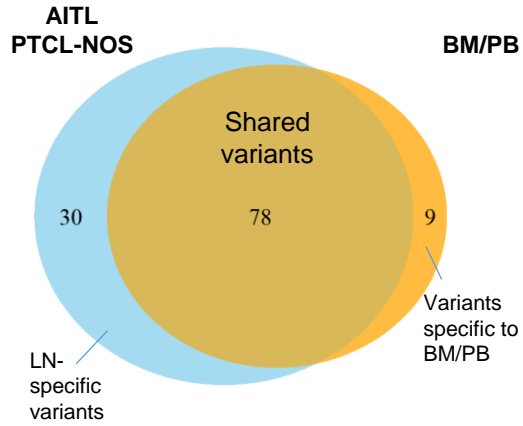
**Suppl. Fig. 5. Summary of all CH-associated and non-CH-associated mutations identified in AITL/PTCL, NOS and their matched BM/PB. Pt#, Patient ID.**

## Reference

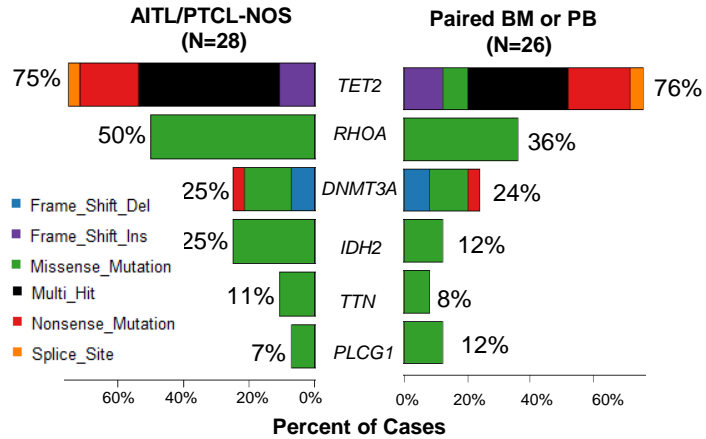
1. Bellanne-Chantelot C, Chaumarel I, Labopin M, et al. Genetic and clinical implications of the Val617Phe *JAK2* mutation in 72 families with myeloproliferative disorders. *Blood*. 2006;108(1):346-352.
2. Beguelin W, Popovic R, Teater M, et al. EZH2 is required for germinal center formation and somatic EZH2 mutations promote lymphoid transformation. *Cancer Cell*. 2013;23(5):677-692.
3. Morin RD, Johnson NA, Severson TM, et al. Somatic mutations altering EZH2 (Tyr641) in follicular and diffuse large B-cell lymphomas of germinal-center origin. *Nat Genet*. 2010;42(2):181-185.
4. Swerdlow SH, Campo E, Pileri SA, et al. The 2016 revision of the World Health Organization classification of lymphoid neoplasms. *Blood*. 2016;127(20):2375-2390.
5. Fiore D, Cappelli LV, Zumbo P, et al. A Novel *JAK1* Mutant Breast Implant-Associated Anaplastic Large Cell Lymphoma Patient-Derived Xenograft Fostering Pre-Clinical Discoveries. *Cancers (Basel)*. 2020;12(6).
6. Cheng S, Singh K, Liu YC, Kluk MJ, Hassane DC, Tam W. Targeted sequencing of recurrently mutated genes in myeloid neoplasms using the Raindance Thunderstorm-Illumina Miseq Platform: My Heme (Myeloid Hematologic Malignancy) Panel. the Association for Molecular Pathology (AMP) 2017 Annual Meeting. Vol. 19: The Journal of Molecular Diagnostics; 2017:962.

Suppl. Fig. 1

A



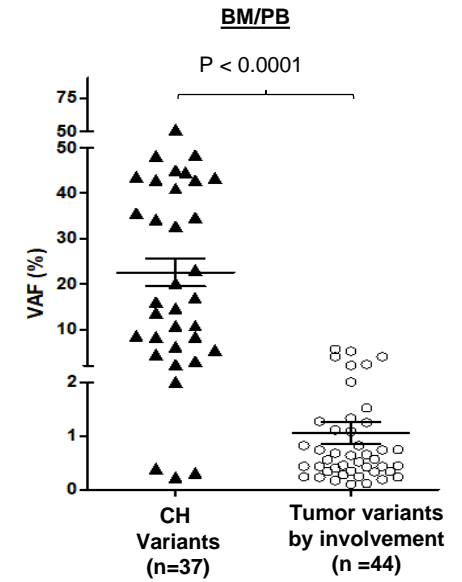
B



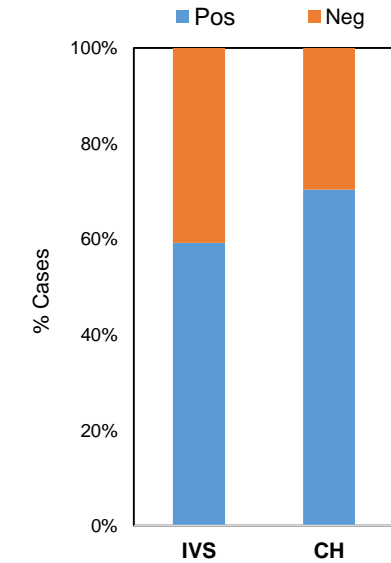
C

Patient ID	BM/PB					TB	CH
	RHOA	IDH2	DNMT3A	TET2_1	TET2_1		
#1	0.43	0	34.62	48.39	0	0.5%	+
#2	0	0	0	0	0	1.5%	+
#3	0	0	0	20.26	16.03	0.0%	+
#4	0.68	1.27	6.22	0.82	0	2.1%	+
#5	0	0.23	48.19	42.79	34.32	1-5%	+
#6	0	0	0	0.39	0	0.0%	+
#7	0.12	0	0	0	0	4.0%	-
#8	0	0	45	43.37	2.61	0.1%	+
#9	0.24	0	0	0	0	1-5%	-
#10	0	0	0	39.26	0.32	0.0%	+
#11	0	0	0	0	0	0.0%	-
#12	0	0	0	1.25	2.29	1-5%	-
#14	0	0	0	32.71	51.49	0.0%	+
#15	0	0	0	44.65	0	1-5%	+
#16	5.21	0	10.85	0	0	10.0%	+
#17	0.44	0	0	0.24	0.66	0.4%	-
#18	0	0	0	3	0	0.0%	+
#19	0	0	0	0	0	1-5%	+
#20	0	0	0	42.29	39.37	0.0%	+
#21	0	0	0	0	0	0.0%	-
#22	0.82	0	0	2.25	0	<1%	+
#23	4	4	0	5.64	0	10.0%	-
#24	0	0	0	41.07	43.65	0.0%	+
#25	0	0	0.24	23.08	0	0.0%	+
#26	0	0	0	0	0	2.1%	-
#28	0	0	0	5.47	10.89	2.4%	+
#29	0.1	0	35.6	0.56	0	1-5%	+

D



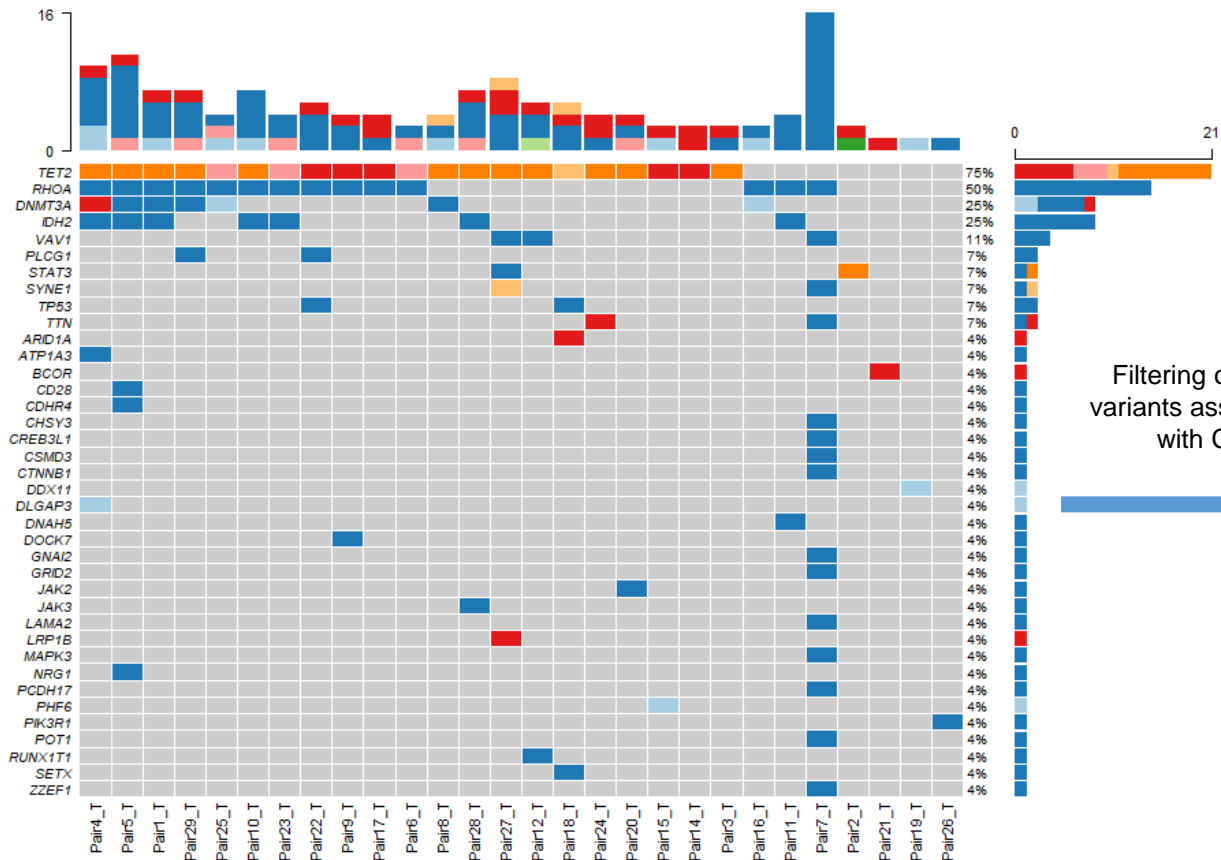
E



# Suppl. Fig.2

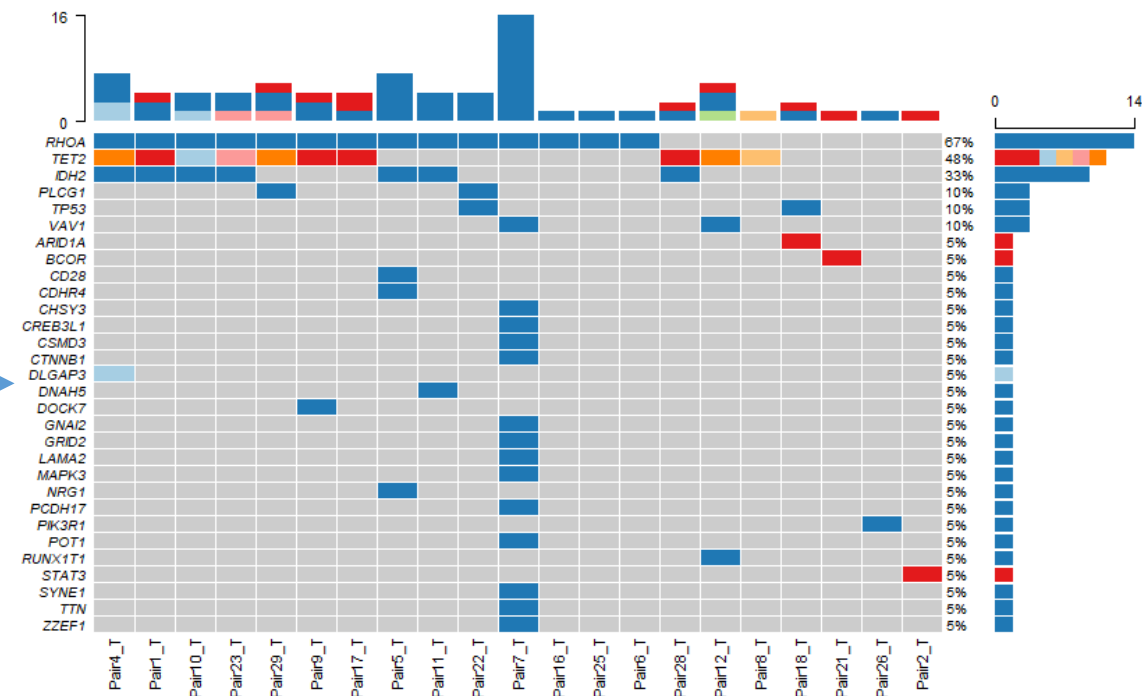
**A**

## Overall genomic alterations (LN, n =28)



**B**

## AITL/PTCL-NOS-specific genomic alterations (LN, n=21)



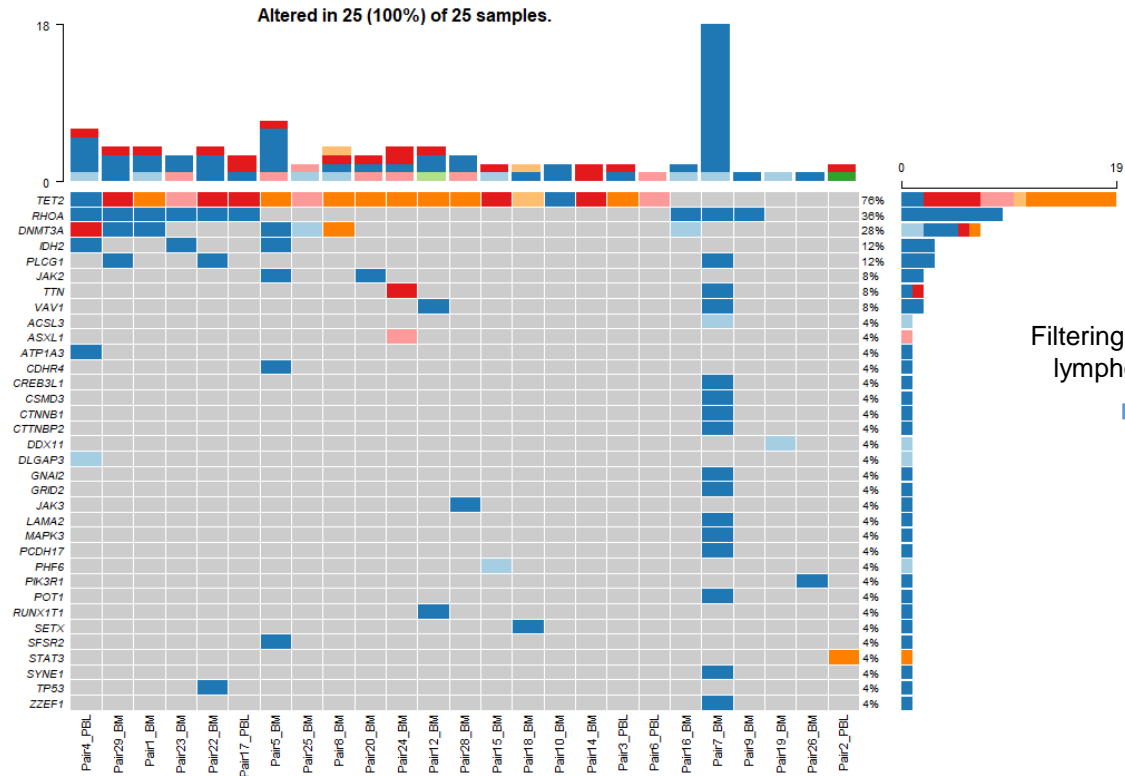
Filtering out the  
variants associated  
with CH



- *Frame\_Shift\_Del*
- *Missense\_Mutation*
- *Nonsense\_Mutation*
- *In\_Frame\_Ins*
- *Frame\_Shift\_Ins*
- *Splice\_Site*
- *In\_Frame\_Del*
- *Multi\_Hit*

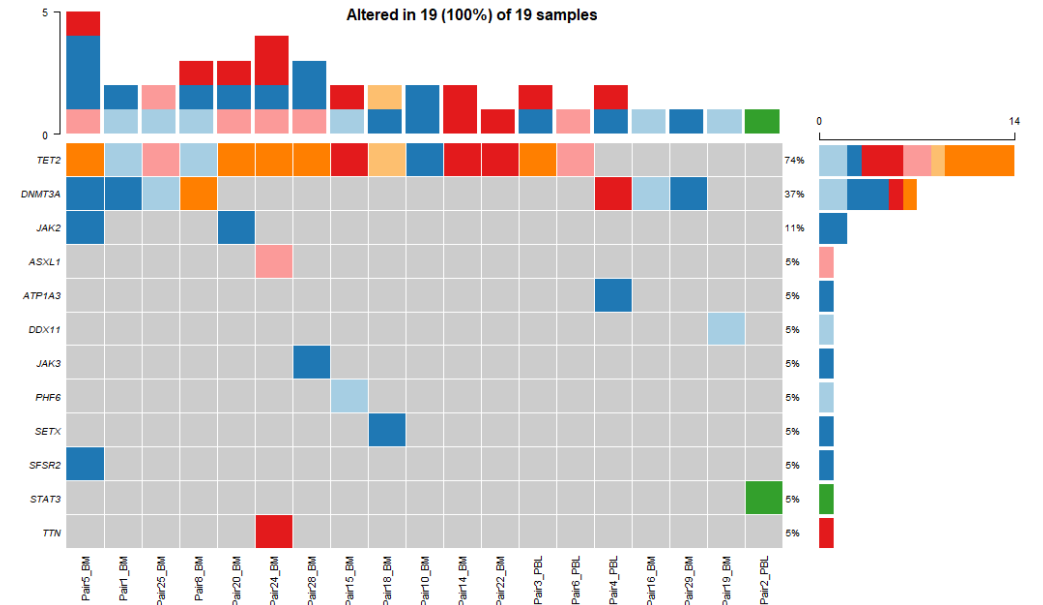
A

Overall genomic alterations  
(paired BM/PB, n =25)



B

CH-associated genomic alterations  
(Paired BM/PB, n =19)



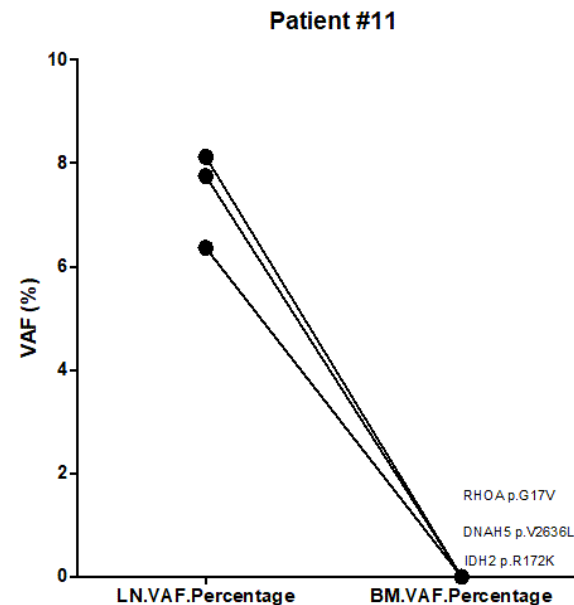
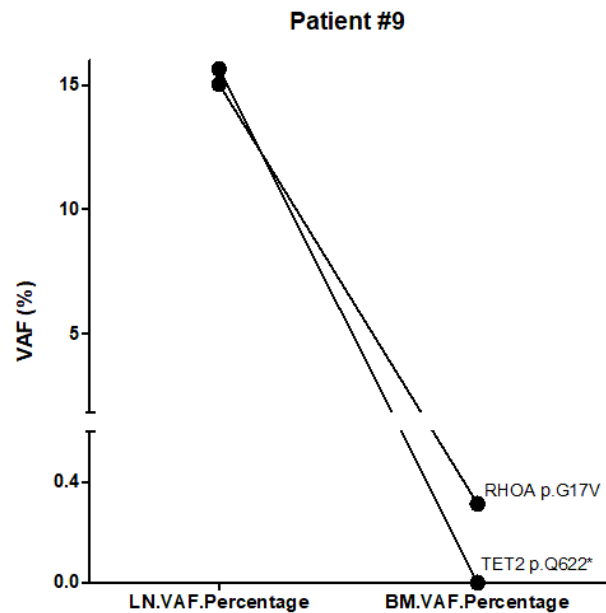
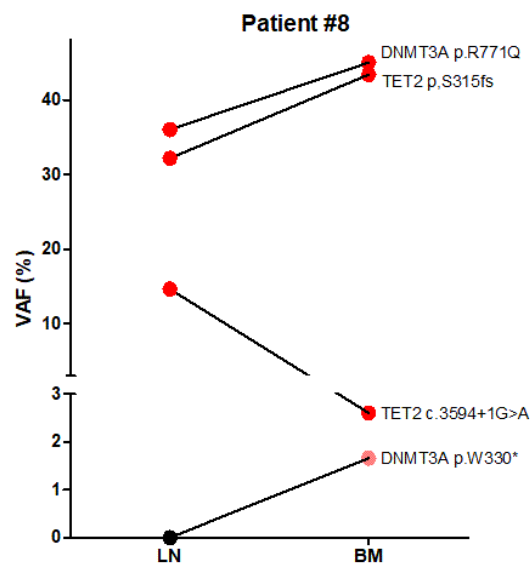
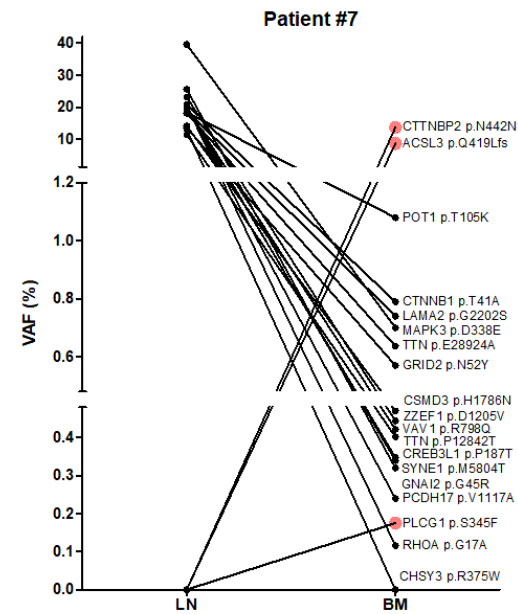
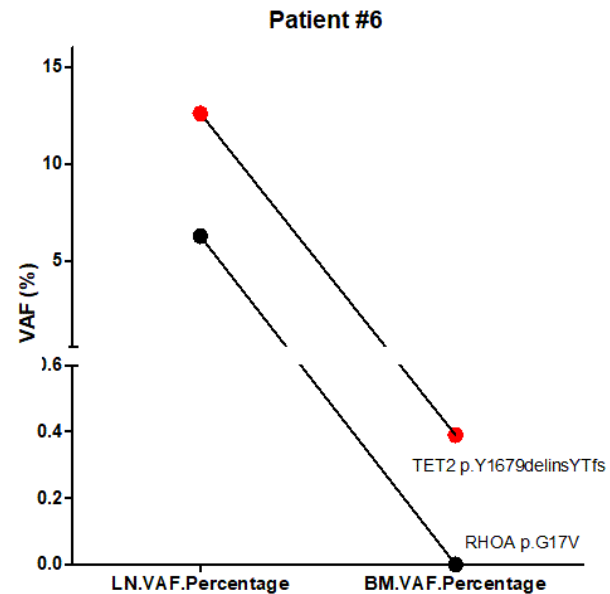
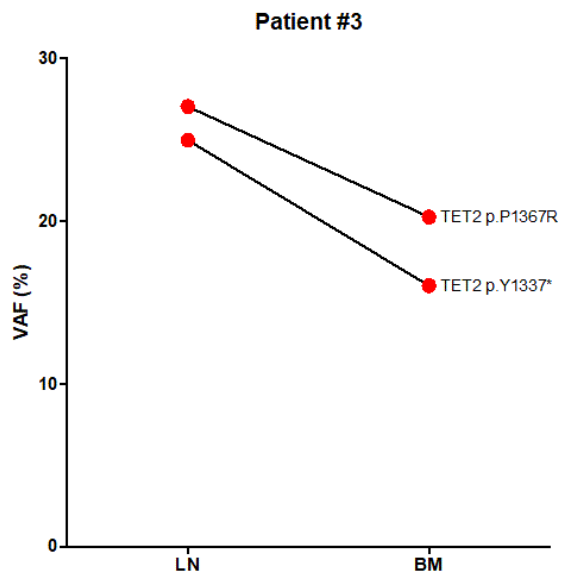
Filtering out the variants by  
lymphoma involvement



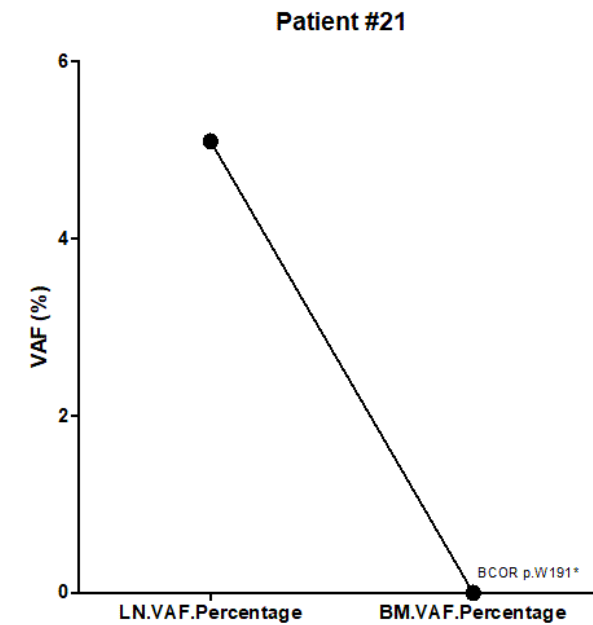
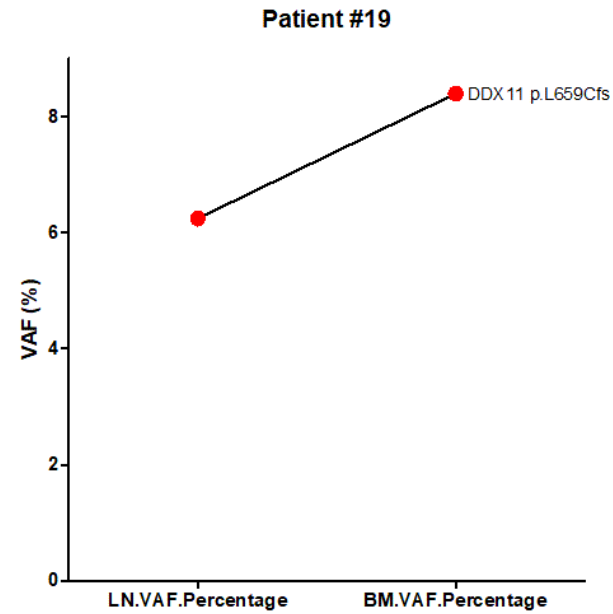
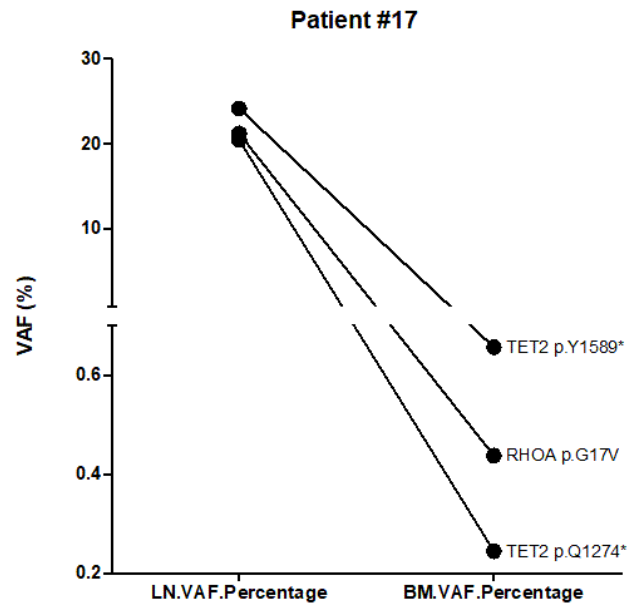
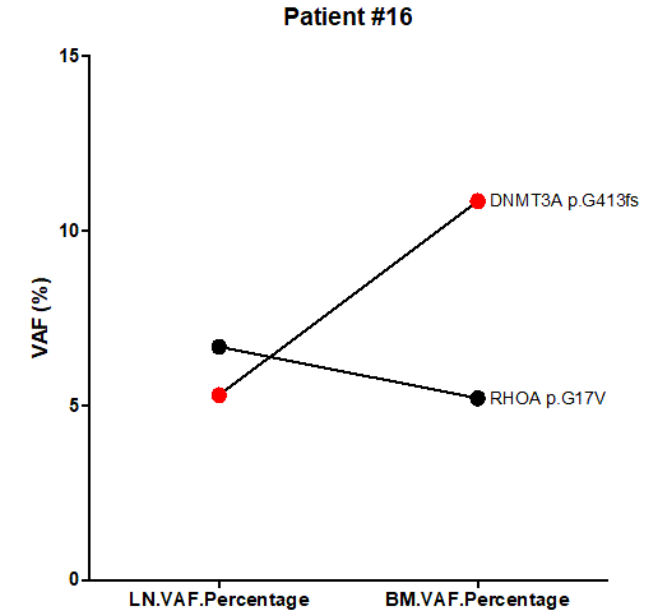
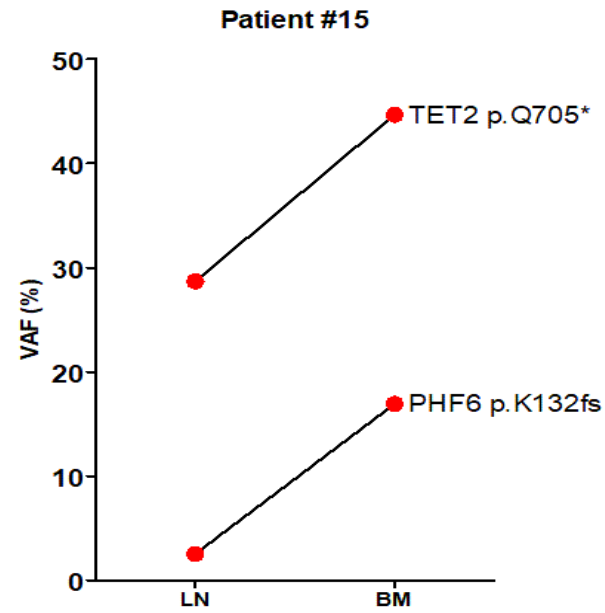
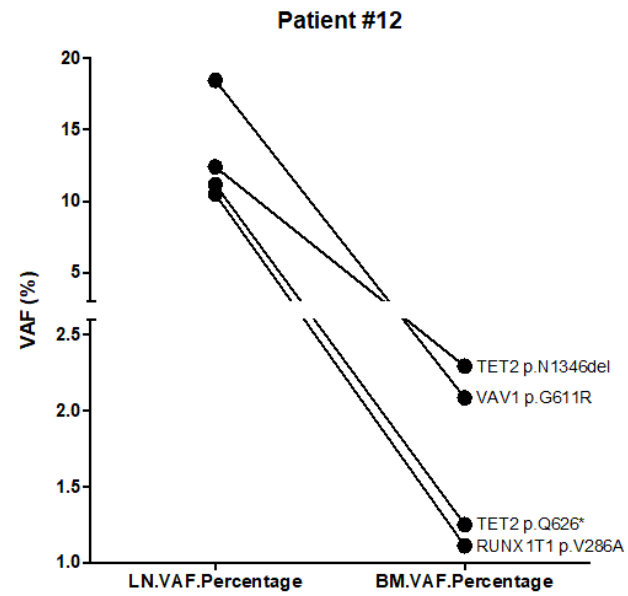
- Frame\_Shift\_Del
- Missense\_Mutation
- Nonsense\_Mutation
- In\_Frame\_Ins
- Frame\_Shift\_Ins
- Splice\_Site
- In\_Frame\_Del
- Multi\_Hit



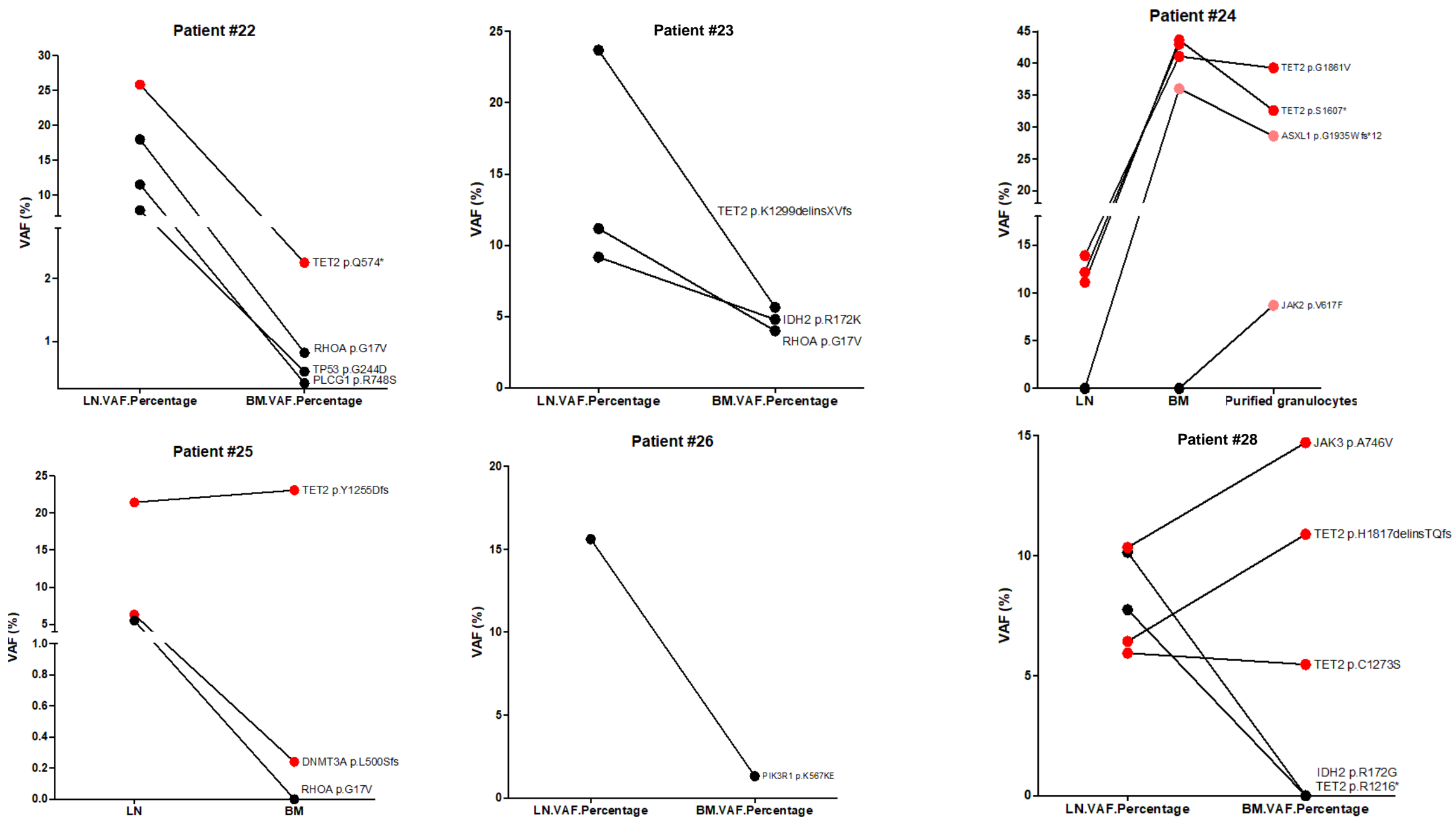
Suppl. Fig. 4 Comparison of VAFs of the variants found in paired AITL and BM/PB samples for each patient (Continued)



Suppl. Fig. 4 Comparing VAFs of the variants found in paired AITL and BM/PB samples for each patient (Continued)



Suppl. Fig. 4 Comparing VAFs of the variants found in paired AITL and BM/PB samples for each patient



Suppl. Fig. 5. Summary of individual mutations shared and unique in neoplastic T cells and untransformed myeloid tissues

	CH-associated mutations			Non-CH-associated mutations				
	Variants	LN	BM/ PB	Pt#	Variants	LN	BM/ PB	Pt#
	TET2 p.E1089fs	36.9	48.4	1#	TET2 p.Q743*	16.7	0	1#
	DNMT3A p.F701L	27.6	34.6	1#	IDH2 p.R172T	20.5	0	1#
	STAT3 p.Y657_K658insALL	21.6	8.3	2#	RHOA p.G17V	14.2	0	1#
	TET2 p.P1367R	27	20.3	3#	STAT3 p.W474*	18.3	0	2#
	TET2 p.Y1337*	25	16	3#	IDH2 p.R172G	8.8	0	4#
	ATP1A3 p.V216M	11.4	4.5	4#	TET2 p.S1812Lfs	7.3	0	4#
	DNMT3A p.Q678*	2	6.2	4#	DLGAP3 p.G85Vfs	6.3	0	4#
	DNMT3A p.W893S	36.1	48.2	5#	RHOA p.G17V	5.5	0	4#
	TET2 p.I274fs	32.1	42.8	5#	TET2 p.R1167K	5.1	0	4#
	TET2 p.L1830*	25.7	34.3	5#	CD28 p.T195P	7.3	0	5#
	TET2 p.Y1679fs	12.6	0.4	6#	CDHR4 p.V647L	10.2	0	5#
	TET2 p.S315fs	32.2	43.4	8#	IDH2 p.R172S	7.1	0	5#
	DNMT3A p.R771N	36	45	8#	NRG1 p.P174L	8.7	0	5#
	TET2 p.D1376G	16.9	0.3	10#	RHOA p.G17V	7.8	0	5#
	TET2 p.N1484K	47.3	39.3	10#	RHOA p.G17V	6.3	0	6#
	TET2 p.K454*	34.5	32.7	14#	CHSY3 p.R375W	13.1	0	7#
	TET2 p.K1799*	35.9	51.5	14#	CREB3L1 p.P187T	20.2	0	7#
	TET2 p.Q705*	28.7	44.7	15#	CSMD3 p.H1788N	14.1	0	7#
	PHF6 p.K132fs	2.6	16.9	15#	CTNNB1 p.T41A	20.9	0	7#
	DNMT3A p.G413fs	5.3	10.9	16#	GNAI2 p.G45R	25.6	0	7#
	SETX p.Y2258D	41.5	2	18#	GRID2 p.N52Y	13.5	0	7#
	TET2 c.3501-1G>A	30.3	3	18#	LAMA2 p.G2202S	19	0	7#
	DDX11 p.L659fs	6.2	8.4	19#	MAPK3 p.D338E	39.6	0	7#
	TET2 p.Q574*	25.9	0.6	22#	PCDH17 p.V1117A	20	0	7#
	TET2 p.G1861V	13.9	41.1	24#	POT1 p.T105K	18.3	0	7#
	TTN p.W25027*	12.2	43	24#	RHOA p.G17A	20.5	0	7#
	TET2 p.S1607*	11.1	43.7	24#	SYNE1 p.M5804T	19.5	0	7#
	TET2 p.Y1255Dfs	21.4	23.1	25#	TTN p.E28924A	18.1	0	7#
	DNMT3A p.L500Sfs	6.3	0.2	25#	TTN p.P12842T	11.4	0	7#
	PTPRZ1 p.D1426fs	68.3	65	26#	VAV1 p.R798Q	19.8	0	7#
	JAK3 p.A746V	10.3	14.7	28#	ZZEF1 p.D1205V	23.1	0	7#
	TET2 p.C1273S	5.9	5.5	28#	ACSL3 p.Q419Lfs	0	8.7	7#
	TET2 p.H1817fs	6.4	10.9	28#	CTTNBP2 p.N442N	0	13.7	7#
	DNMT3A p.R882H	46	35.6	29#	TET2 c.3594+1G>A	14.6	0	8#
					TET2 p.Q822*	15.7	0	9#
					RHOA p.G17V	15	0	9#
					DOCK7 p.F240S	11.2	0	9#
					TET2 p.V415fs	16.6	0	10#
					RHOA p.G17V	10.9	0	10#
					IDH2 p.R172T	10	0	10#
					RHOA p.G17V	6.4	0	11#
					DNAH5 p.V2838L	8.1	0	11#
					IDH2 p.R172K	7.8	0	11#
					RUNX1T1 p.V286A	10.5	0	12#
					TET2 p.Q828*	11.2	0	12#
					TET2 p.N1348del	12.4	0	12#
					VAV1 p.G811R	18.4	0	12#
					RHOA p.G17V	6.7	0	16#
					RHOA p.G17V	21.2	0	17#
					TET2 p.Q1274*	20.4	0	17#
					TET2 p.Y1589*	24.1	0	17#
					TP53 p.P151T	47.2	0	18#
					ARID1A p.G779*	14.1	0	18#
					BCOR p.W191*	5.1	0	18#
					TP53 p.G244D	7.8	0	22#
					PLCG1 p.R748S	11.5	0	22#
					RHOA p.G17V	18	0	22#
					IDH2 p.R172K	9.2	0	23#
					RHOA p.G17V	11.2	0	23#
					TET2 p.K1299fs	23.7	0	23#
					RHOA p.G17V	5.5	0	25#
					PIK3R1 p.K587KE	15.6	0	26#
					IDH2 p.R172G	10.1	0	28#
					TET2 p.R1216*	7.8	0	28#
					PLCG1 p.S520F	12.5	0	29#
					RHOA p.G17VG	10.9	0	29#
					TET2 p.L1111*	11.8	0	29#
					TET2 p.C1211fs	12.4	0	29#



Supplemental Table 1 Patient characteristic

No.	Patient ID	Type of Specimens	Sex	Age	Dx	Pathology of BM/PBL	Concurrent hematologic Malignancy	Morphology	MFC	TCRG Rearrangement	TB
1	#1	BM	F	58	Lung cancer, AITL	megakaryocytes slightly increased in number without significant cytologic atypia. PBL Normocytic anemia. Leukocytosis with neutrophilia	No	+	0.5%	n/a	0.5%
2	#2	PBL	M	33	PTCL, NOS	BM, hypocellular bone marrow with relative eosinophilia, PBL, eosinophilia	No	-	1.50%	PCR+	1.5%
3	#3	PBL	M	51	AITL	unremarkable	No	-	0	PCR-	0.0%
4	#4	BM	F	65	AITL	involvement, megakaryocytes are focally clustered and some have atypical nuclear lobation, PBL, unremarkable	No	+	2.10%	PCR+	2.1%
5	#5	BM	F	65	AITL	granulopoiesis, dysgranulopoiesis, decreased erythropoiesis, monocytosis, unremarkable T cells. PBL, Absolute monocytosis.	CMMML, 10 months post-AITL Dx	-	0	PCR+	1-5% <sup>§</sup>
6	#6	PBL	M	75	AITL	Megakaryocytes were dysplastic (>10%). Including small / giant forms with hypo / hyperlobulated nuclei. Myelopoiesis is hyperplastic and slightly left-shifted. Mild dysgranulopoiesis is present (<10%) with giant forms and abnormal segmentation.	No	-	0	n/a	0.0%
7	#7	BM	M	70	AITL	involvement	No	+	4%	n/a	4.0%
8	#8	BM	M	72	Prostate cancer, PTCL-TFH	involvement	No	+	0.10%	n/a	0.1%
9	#9	BM	F	53	AITL	unremarkable	No	-	0	PCR+	1-5% <sup>§</sup>
10	#10	BM	M	63	AITL	unremarkable	No	-	0	PCR-	0.0%
11	#11	BM	F	70	AITL	ITP	No	-	0	PCR-	0.0%
12	#12	PBL	M	75	AITL	unremarkable	No	-	0	PCR+	1-5%
13	#14	BM	M	77	PTCL-TFH, DLBCL	ITP	DLBCL, 7 years post-AITL Dx	-	0	PCR-	0.0%
14	#15	BM	M	76	AITL	unremarkable	No	-	0	PCR+	1-5% <sup>§</sup>
15	#16	BM	F	84	AITL	involvement	No	+	10%	PCR+	10.0%
16	#17	PBL	M	80	AITL	involvement	No	-	0.40%	PCR+	0.4%
17	#18	BM	M	63	PTCL, NOS	Mildly hypercellular marrow with mild granulocytic hyperplasia	No	-	0	PCR-	0.0%
18	#19	BM	F	53	AITL	unremarkable	No	-	0	PCR+	1-5% <sup>§</sup>
19	#20	BM	M	45	Lung Cancer, post-PV MF, PTCL-TFH	post-PV myelofibrosis	PV, post-PV myelofibrosis prior to AITL Dx	-	0	PCR-	0.0%
20	#21	BM	F	42	AITL	unremarkable	No	-	0	PCR-	0.0%
21	#22	BM	F	63	AITL	a mildly hypercellular bone marrow with myeloid hyperplasia	No	-	0	PCR-	<1%
22	#23	BM	M	65	DLBCL and AITL	unremarkable	DLBCL	+	10%	PCR+	10.0%
23	#24	BM	M	38	AITL	Myelopoiesis is hyperplastic and slightly left-shifted with ~4% blasts. Evidence of significant dysplasia is not seen	No	-	0	PCR-	0.0%
24	#25	BM	M	70	AITL	Hypercellular bone marrow with myeloid hyperplasia	No	-	0	PCR-	0.0%
25	#26	BM	M	63	PTCL-TFH	involvement	No	+	2.10%	PCR+	2.1%
26	#27	no matched BM or PBL	F	67	Lung cancer, PTCL, NOS	n/a	n/a	n/a	n/a	n/a	n/a
27	#28	BM	F	79	AITL	involvement	No	+	2.40%	PCR+	2.4%
28	#29	BM	M	58	CTCL to AITL	small population of abnormal myeloid blasts noted in BM, but no MPN diagnosed	No	-	0	PCR+	1-5% <sup>§</sup>

PT#, Patient ID, T, type of specimen, HP, histopathology  
 IM, immunophenotyping, MP, molecular pathology testing  
 TB, neoplastic T cell burden by BM involvement  
 CH, clonal hematopoiesis  
 IC, suspicious but inconclusive  
 § limit of detection of TCRG (1-5%)  
 n/a, data unavailable  
 DLBCL, diffuse large B cell lymphoma  
 CMMML, Chronic Myelomonocytic Leukemia  
 PCR+, monoclonal TCR rearrangement  
 AITL, angioimmunoblastic T-cell lymphoma  
 PTCL, peripheral T-cell lymphoma  
 CTCL, cutaneous T-cell lymphoma  
 MF, myelofibrosis  
 MCF, multiple color flow cytometry

**Supplemental Table 2 Variant summary**

		Primary AITL lymphoma				Paired BM/PBL <sup>§</sup>			
		summary	Mean	Median	Percent	summary	Mean	Median	Percent
Variant Classification	Frame_Shift_Del	9	0.333	0	8.82	6	0.316	0	13.64
	Frame_Shift_Ins	7	0.259	0	6.86	7	0.316	0	15.91
	In_Frame_Del	1	0.037	0	0.98	0	0	0	0.00
	In_Frame_Ins	1	0.037	0	0.98	1	0.053	0	2.27
	Missense_Mutation	62	2.296	1	60.78	17	0.789	1	38.64
	Nonsense_Mutation	20	0.741	1	19.61	12	0.579	0	27.27
	Splice_Site	2	0.074	0	1.96	1	0.053	0	2.27
Total		102	3.778	3	100.00	44	2.105	2	100.00
No. of Samples		27				27*			
No. of Mutated genes		37				14			

\*A total of 23 bone marrow and 4 PBL samples were sequenced. Among 27 BM/PB samples, 20 had identifiable mutated genes after filtering out the variants involved.

<sup>§</sup> the variants from the involved lymphoma excluded

Supplemental Table3 Individual mutations and their VAFs in the lymphoma cases and matched BM/PB

No. of Patient	Patient ID	Dx	Mutations	Alt% in lymphoma (LN)	Alt% in BM or PBL	Purified granulocytes from PB of AITL patients	Note
1	Patient 1#	Lung cancer, AITL	TET2 p.E1089fs DNMT3A p.F701L TET2 p.Q743* IDH2 p.R172T RHOA p.G17V	36.87 27.59 16.69 20.47 14.17	48.39 34.62 0.43 0.00 0.43		
2	Patient 2#	PTCL, NOS	STAT3 p.Y657_K658insALL STAT3 p.W474*	21.61 18.33	8.34 2		
3	Patient 3#	AITL	TET2 p.P1367R TET2 p.Y1337*	27.04 24.97	20.26 16.03		
4	Patient 4#	AITL	ATP1A3 p.V216M IDH2 p.R172G TET2 p.S1612Lfs DLGAP3 p.G85Vfs RHOA p.G17V TET2 p.R1167K DNMT3A p.Q678*	11.38 8.81 7.34 6.27 5.53 5.11 1.95	4.47 1.27 0 1.52 0.68 0.82 6.22		
5	Patient 5#	AITL	CD28 p.T195P CDHR4 p.V647L DNMT3A p.W893S IDH2 p.R172S JAK2 p.V617F SRSF2 NRG1 p.P174L RHOA p.G17V TET2 p.I274delinsISfs TET2 p.L1830*	7.32 10.15 36.08 7.08 0.00 0.00 8.70 7.79 32.13 25.66	0.00 0.28 48.19 0.23 3.00 28.00 0.00 0.00 42.79 34.32		
6	Patient 6#	AITL	TET2 p.Y1679delinsYTfs RHOA p.G17V	12.6 6.28	0.39 0.00		
7	Patient 7#	AITL	CHSY3 p.R375W CREB3L1 p.P187T CSMD3 p.H1786N CTNNB1 p.T41A GNAI2 p.G45R GRID2 p.N52Y LAMA2 p.G2202S MAPK3 p.D338E PCDH17 p.V1117A PLCG1 p.S345F POT1 p.T105K RHOA p.G17A SYNE1 p.M5804T TTN p.E28924A TTN p.P12842T VAV1 p.R798Q ZZEF1 p.D1205V ACSL3 p.Q419Lfs CTTNBP2 p.N442N	13.06 20.21 14.13 20.86 25.62 13.51 18.97 39.61 19.96 0 18.3 20.48 19.46 18.11 11.4 19.81 23.15 0 0	0 0.34 0.46 0.75 0.34 0.57 0.74 0.743034056 0.239616613 0 1.080351114 0.116009281 0.347912525 0.636942675 0.401854714 0.421545667 0.443951165 8.66 13.66204417		
8	Patient 8#	Prostate cancer PTCL-TFH	TET2 p.S315fs TET2 c.3594+1G>A DNMT3A p.Arg771Gln DNMT3A p.Trp330*	32.17 14.64 36 0	43.37349398 2.605459057 45 1.66		
9	Patient 9#	AITL	TET2 p.Q622* RHOA p.G17V DOCK7 p.P240S	15.65 15.04 11.19	0 0.241400121 0		
10	Patient 10#	AITL	TET2 p.D1376G TET2 p.V415fs RHOA p.G17V IDH2 p.R172T TET2 p.N1484K	16.89 16.62 10.92 10.02 47.33	0.31512605 0 0 0 38.26		
11	Patient 11#	AITL	RHOA p.G17V DNAH5 p.V2636L IDH2 p.R172K	6.36 8.12 7.75	0 0 0		
12	Patient 12#	AITL	RUNX1T1 p.V286A TET2 p.Q626* TET2 p.N1346del VAV1 p.G611R	10.49 11.17 12.4 18.45	1.11 1.25 2.29 2.09		

13	Patient 14#	PTCL-TFH DLBCL	TET2 p.K454* TET2 p.K1799* EZH2 p.Y646S	34.50 35.94 0.00	32.71 51.49 0.00		41.8 <sup>&amp;</sup> 33.6 <sup>&amp;</sup> 29.9 <sup>&amp;</sup>
14	Patient 15#	AITL	TET2 p.Q705* PHF6 p.K132fs	28.68 2.56	44.65 16.94		
15	Patient 16#	AITL	DNMT3A p.G413fs RHOA p.G17V	5.30 6.68	10.85 5.21		
16	Patient #17	AITL	RHOA p.G17V TET2 p.Q1274* TET2 p.Y1589*	21.2 20.44 24.14	0.44 0.24 0.66		
17	Patient #18	PTCL, NOS	ARID1A p.G779* SETX p.Y2258D TET2 c.3501-1G>A TP53 p.P151T	14.08 41.47 30.3 47.38	0 2 3 0		
18	Patient #19	AITL	DDX11 p.L659Cfs	6.24	8.39		
19	Patient #20	Lung Cancer post-PV MF PTCL-TFH	TET2 p.Q939* TET2 p.E1026delinsXDfs JAK2 p.V617F	36.59 19.64 54.48	42.29 39.37 88		
20	Patient #21	AITL	BCOR p.W191*	5.1	0		
21	Patient #22	AITL	RHOA p.G17V TET2 p.Q574* TP53 p.G244D PLCG1 p.R748S	17.99 25.85 7.83 11.51	0.82 2.25 0.52 0.33		
22	Patient #23	DLBCL AITL	IDH2 p.R172K RHOA p.G17V TET2 p.K1299delinsXVfs	9.17 11.17 23.69	4 4 5.64		
23	Patient #24	AITL	TET2 p.G1861V TTN p.W25027* TET2 p.S1607* JAK2 p.V617F ASXL1 p.G646Wfs*12	13.9 12.17 11.12 0 0	41.07 43 43.65 0 36	39.3 n/a 32.6 8.7 28.6	
24	Patient #25	Prostate cancer HL AITL	DNMT3A p.L500Sfs RHOA p.G17V TET2 p.Y1255Dfs	6.29 5.5 21.44	0.24 0 23.08		
25	Patient #26	PTCL-TFH	PIK3R1 p.K567KE	15.61	1.33		
26	Patient #27	PTCL, NOS Lung cancer	LRP1B p.L2470* STAT3 p.E616G TET2 p.K1254* TET2 p.C1289F SYNE1 c.4977-2delA VAV1 p.D797DV	1 6.55 18.51 17.36 20.88 29.85	n/a n/a n/a n/a n/a n/a		
27	Patient #28	AITL	IDH2 p.R172G JAK3 p.A746V TET2 p.R1216* TET2 p.C1273S TET2 p.H1817delinsTQfs	10.14 10.34 7.75 5.94 6.43	0 14.71 0 5.47 10.89		
28	Patient 29#	AITL	PLCG1 p.S520F RHOA p.G17VG TET2 p.L1111* TET2 p.C1211delinsLFfs DNMT3A p.R882H	12.52 10.86 11.82 12.37 46	0.19 0.1 0.56 0 35.6		

LN, lymph node  
BM, bone marrow  
PBL, peripheral blood  
VAF, variant allele frequency  
DLBCL, diffuse large B cell lymphoma  
Vaf values highlighted in yellow represent those of the AITL mutations involved in bone marrow  
Vaf values highlighted in pink represent those of the mutations found only in bone marrow  
<sup>&</sup> detected in DLBCL (renal tissue) by myeloid panel  
n/a, no data available  
PV, polycythemia vera  
MF, myelofibrosis  
TFH, follicular T helper cell  
Alt%, alternate allele frequency  
Alt% highlighted in yellow represent those of the AITL mutations involved in bone marrow  
Alt% highlighted in pink represent those of the mutations found only in bone marrow